JPET Fast Forward. Published on July 22, 2016 as DOI: 10.1124/jpet.116.233114
This article has not been copyedited and formatted. The final version may differ from this version.

In vivo characterization of the ultrapotent monoacylglycerol lipase inhibitor {4-[bis-(benzo[d][1,3]dioxol-5-yl)methyl]-piperidin-1-yl}(1*H*-1,2,4-triazol-1-yl)methanone (JJKK-048)

Niina Aaltonen, Ewa Kedzierska, Jolanta Orzelska-Górka, Marko Lehtonen, Dina Navia-Paldanius, Hermina Jakupovic, Juha Savinainen, Tapio Nevalainen, Jarmo T. Laitinen, Teija Parkkari, Mikko Gynther

School of Medicine, Institute of Biomedicine/Physiology, University of Eastern Finland, Kuopio, Finland (N.A., D.N-P., H.J., J.S., J.T.L.)

Department of Pharmacology and Pharmacodynamics, Faculty of Pharmacy with Division of Medical Analytics, Medical University of Lublin, Lublin, Poland (E.K., J.O-G.)

School of Pharmacy, University of Eastern Finland, Kuopio, Finland (M.L., T.N., T.P., M.G.)

Running title: *In vivo* characterization of the compound JJKK-048

Corresponding author: Niina Aaltonen**,** Institute of Biomedicine/Physiology, University of Eastern Finland, P.O. Box 1627, FI-70211 Kuopio, Finland

E-mail: Niina Aaltonen@uef.fi, Tel: +358-40-3553865, Fax: +358-17-163032

Number of text pages: 41

Number of figures: 7

Number of tables: 1

Number of references: 52

Number of words in Abstract (max 250): 218

Number of words in Introduction (max 750): 728

Number of words in Discussion (max 1500): 1500

Abbreviations: 2-AG, 2-arachidonoylglycerol; ABHD, α/β-hydrolase domain containing protein; ABPP, activity based protein profiling; AEA, anandamide; CES, carboxylesterase; ES1, carboxylesterase 1; FAAH, fatty acid amide hydrolase; HP-β-CD, 2-hydroxypropyl-β-cyclodextrin; JJKK-048, {4-[bis-(benzo[d][1,3]dioxol-5-yl)methyl]-piperidin-1-yl}(1*H*-1,2,4-triazol-1-yl)methanone; JZL184, 4-nitrophenyl 4-(dibenzo[d][1,3]dioxol-5-yl(hydroxy)methyl)piperidine-1-carboxylate; KML29, 1,1,1,3,3,3-hexafluoropropan-2-yl 4-(bis(benzo[*d*][1,3]dioxol-5-yl)(hydroxy)methyl) piperidine-1-carboxylate; LC-MS/MS, Liquid chromatography-tandem mass spectrometry; MAGL, monoacylglycerol lipase; MPE, maximum possible effect; PEG, polyethylene glycol; Rimonabant, 5-(4-Chlorophenyl)-1-(2,4-dichloro-phenyl)-4-methyl-N-(piperidin-1-yl)-1H-pyrazole-3-carboxamide; SAR629, (4-(Bis(4-fluorophenyl)methyl)piperazin-1-yl)(1*H*-1,2,4-triazol-1-yl)-methanone hydrochloride; URB602, biphenyl-3-ylcarbamic acid cyclohexyl ester

Section: Neuropharmacology

Abstract

Monoacylglycerol lipase (MAGL) is a serine hydrolase that acts as a principal degradative enzyme for the endocannabinoid 2-arachidonoylglycerol (2-AG). In addition to terminating the signaling function of 2-AG, MAGL liberates arachidonic acid to be used as primary source for neuroinflammatory prostaglandin synthesis in brain. MAGL activity also contributes in cancer pathogenicity by producing precursors for tumor-promoting bioactive lipids. Pharmacological inhibitors of MAGL provide valuable tools for characterization of MAGL and 2-AG signaling pathways. They also hold great therapeutic potential to treat several pathophysiological conditions, such as pain, neurodegenerative disorders as well as cancer. We have previously reported piperidine triazole urea, {4-[bis-(benzo[d][1,3]dioxol-5-yl)methyl]-piperidin-1-yl}(1*H*-1,2,4-triazol-1-yl)methanone (JJKK-048), to be an ultrapotent and highly selective inhibitor of MAGL *in vitro.* Here we characterize *in vivo* effects of JJKK-048. Acute *in vivo* administration of JJKK-048 induced a massive increase in mouse brain 2-AG levels without affecting brain anandamide levels. JJKK-048 appeared to be extremely potent *in vivo*. Activity-based protein profiling (ABPP) revealed that JJKK-048 maintains good selectivity towards MAGL over other serine hydrolases. Our results also showed for the first time that JJKK-048 promoted significant analgesia in writhing test with the low dose that did not cause cannabimimetic side effects. At high dose of JJKK-048 induced analgesia both in writhing test and in tail immersion test, as well as hypomotility and hyperthermia but not catalepsy.

Introduction

Endocannabinoids are lipid-structured signaling molecules that act as natural ligands for cannabinoid CB_1 and CB_2 receptors, which also are the targets of the psychoactive component of *Cannabis Sativa*. The two most intensively studied endocannabinoids are 2-arachidonoylglycerol (2-AG) and anandamide (AEA) (Devane et al., 1992; Mechoulam et al., 1995; Sugiura et al., 1995). Generally, endocannabinoids are synthesized on demand from plasma membrane phospholipid precursors and after exerting their effect by activating specific receptors, they are rapidly degraded by enzymatic activity. The principal brain endocannabinoid is 2-AG which regulates central nervous system development and synaptic plasticity (Bisogno et al., 1999; Berghuis et al., 2007; Hashimotodani et al., 2007). Endocannabinoids also regulate cognition, emotional functions, and food intake and are involved in several pathophysiological processes including pain and neurodegenerative diseases (Di Marzo and Petrosino, 2007; Sugiura, 2009; Pacher et al., 2006). For therapeutic purposes, direct activation of cannabinoid receptors, however, has proved to be challenging due to the side effects affecting cognition and motor control (Pacher and Kunos, 2013).

Monoacylglycerol lipase (MAGL) is a serine hydrolase that catalyzes the hydrolysis of monoacylglycerols to their corresponding fatty acids and glycerol (Karlsson et al., 1997; Dinh et al., 2002; Dinh et al., 2004; Saario et al., 2004). MAGL has been suggested to be the main hydrolase terminating 2-AG actions in the brain, accounting for ~85 % of total 2-AG hydrolysis at the bulk brain level (Blankman et al., 2007). The remaining ~15 % has been attributed mainly to two α/β-hydrolase domain (ABHD) containing proteins, ABHD6 and ABHD12 (Blankman et al., 2007; Savinainen et al., 2012). According to recent studies, in

addition to regulating synaptic 2-AG signaling, MAGL have been demonstrated to play a key role in controlling brain eicosanoid production. Notably, MAGL-catalyzed hydrolysis of 2-AG liberates arachidonic acid to be used as precursor for the production of neuroinflammatory prostaglandins (Nomura et al., 2011). The pharmacological or genetic inactivation of MAGL has attenuated neuroinflammation and exerted neuroprotective effects in mouse models of neurodegenerative diseases (Nomura et al., 2011; Chen et al., 2012; Piro et al., 2012). Moreover, MAGL contributes to cancer pathogenicity by providing free fatty acids for the production of tumor-promoting bioactive lipids such as lysophosphatidic acid and prostaglandins (Nomura et al., 2011). Thus, pharmacological inhibitors of MAGL may have great therapeutic potential both by locally enhancing 2-AG levels and by reducing arachidonic acid-derived lipid production.

Several types of compounds have been reported to inhibit MAGL but only few compounds represent sufficient selectivity and potency enabling their use *in vivo*. Especially important is to achieve selectivity between MAGL and fatty acid amide hydrolase (FAAH), the primary enzyme responsible for the degradation of AEA (Deutsch and Chin, 1993), since dual inhibition of MAGL and FAAH have been demonstrated to induce behavioral effects similar to those achieved with direct CB_1 receptor agonists, including catalepsy (Long et al., 2009a). The sulfhydryl reagent *N*-arachidonoylmaleimide (Saario et al., 2005; Burston et al., 2008) and a carbamate compound URB602 (Hohmann et al., 2005) were among the first compounds showing activity *in vivo* but their potency and MAGL selectivity was proved to be insufficient. More recently, the carbamate compounds JZL184 (Long et al., 2009b) and its derivative KML29 (Chang et al., 2012) were reported as selective MAGL inhibitors that increase brain 2-AG levels and display more restricted set of behavioral effects when compared to the CB_1 agonists or the dual MAGL and FAAH inhibitors. Carbamate-based

inhibitors typically inactivate serine hydrolases by an irreversible covalent modification (carbamoylation) of the catalytic serine nucleophile (Alexander and Cravatt, 2005; Bar-On et al., 2002).

We have characterized piperazine and piperidine triatzole ureas as potent and selective inhibitors of MAGL (Aaltonen et al., 2013). Our work culminated in the synthesis of compound JJKK-048, which is *in vitro* the most potent and MAGL-selective inhibitor currently available. In the present study, we extend our initial study by testing the *in vivo* effects of JJKK-048. We provide evidence that JJKK-048 exhibits extremely high potency in inhibiting MAGL in brain and peripheral tissues and also maintains good selectivity over other serine hydrolases. We observed that acute administration of JJKK-048 remarkably increased mouse brain 2-AG levels without affecting AEA levels. According to behavioral experiments, JJKK-048 induced antinociception and dose-dependent hypomotility and hypothermia but no catalepsy. Among these *in vivo* effects, only antinociceptive effect of JJKK-048 was blocked by rimonabant, suggesting also other than CB1 mediated effects of JJKK-048 in behavioral tests.

Materials and methods

Drugs

JJKK-048 and JZL184 were synthesized at School of Pharmacy, University of Eastern Finland, Kuopio, Finland. Rimonabant was purchased from Tocris Bioscience (Bristol, UK) and WIN 55,212-2 from Sigma Chemicals (St. Louis, USA). Fluorophosphonate probe TAMRA-FP (ActivX Fluorophosphonate Probes) was from Thermo Fisher Scientific (Rockford, IL, USA). Endocannabinoid standard solutions and deuterated internal standards were purchased from Cayman Chemicals (Ann Arbor, MI, USA). All the other chemicals were of the finest purity available.

Animals

In vivo MAGL inhibition experiments were performed on male C57BL/6JOlaHsd mice (8 week-old, weight 20-26 g) that were obtained from the National Laboratory Animal Centre, University of Eastern Finland, Kuopio, Finland. Mice were housed under standard laboratory conditions (12-12 h light-dark cycle, food and water *ad libitum*, 60 % relative humidity). The experiments were performed according to appropriate European community guidelines and Guide for the Care and Use of Laboratory Animals (National Institutes of Health publication no. 85-23, revised in 1985). The procedures were reviewed and approved by the Finnish National Animal Experiment Board. The behavioral experiments were performed on male Albino Swiss mice (weight 20-30 g), where 6-8 animals were kept in a cage, at room temperature (22 ± 1 °C), under a 12-12 h light-dark cycle with free access to food (LSM, Poland) and water. All behavioral experiments were carried out according to the National

Institute of Health Guidelines for the Care and Use of Laboratory Animals and to the European Community Directive for the Care and Use of Laboratory of 24 November 1986 (86/609/EEC), and approved by the Local Ethics Committee for Animal Experimentation (14/2014).

In vivo administration of the studied compounds

JJKK-048 was dissolved in 5% (v/v) DMSO in gently heated 10% (w/v) 2-hydroxypropyl-β-cyclodextrin (HP-β-CD) (Sigma Chemicals, St. Louis, USA) and injected intraperitoneally (i.p.) in a volume of 10 ml/kg. After the indicated dosing regimens, the mice were sacrificed by decapitation and tissues were immediately frozen in liquid nitrogen. In behavioral experiments, JJKK-048 was dissolved in 5% (v/v) DMSO in gently heated 10% (w/v) HP-β-CD (control I) and injected i.p. 30 min before the tests. JZL184 was dissolved by vortexing, sonicating and gentle heating directly into 4:1 v/v PEG 300/ Tween 80 (control II) (Long et al., 2009b) and administered i.p. 120 min before the tests. Rimonabant and WIN 55,212-2 were suspended in one drop of 1 % solution of Tween 80 (Sigma Chemicals, St. Louis, USA), diluted in saline (0.9 % NaCl). Rimonabant was administered via i.p. injection, 10 min prior to JJKK-048 exposure. In the tail immersion WIN 55,212-2 was injected 30 min before the tail immersion. In 'writhing' procedure, the tested substances were subcutaneously (s.c.) injected and the acetic acid (0.6 % solution) was i.p. administered. All the substances were given in a volume of 10 ml/kg. Each experimental group consisted of 6-8 animals per dose and all the animals were used only once. The control animals received an equivalent volume of corresponding vehicle at the respective time before the tests.

ABPP of serine hydrolases

Frozen brains and selected peripheral tissues were first homogenized with Qiagen TissueLyser II (3 min with frequency 30 1/s) to obtain fine tissue powder. Then, approximately 20-80 mg of frozen tissue powder was weighted into microcentrifuge tubes and further ground in Tris-buffer (50 mM Tris–HCl [pH 7.4], 150 mM NaCl, ml per mg powder) with plastic homogenizer, and thereafter, centrifuged at low speed (1000*g*, 10 min, +4 °C). The resulting supernatant containing both soluble and membrane fractions (a homogenate fraction), was removed for storage at −80 °C. Protein concentration was measured using Pierce BCA Protein Assay Kit (Pierce, Rockford, IL) with bovine serum albumin as a standard.

ABPP was performed using TAMRA-FP, an activity-based fluorophosphonate probe reporting activity of serine hydrolases, as previously described (Aaltonen et al., 2013). Briefly, 100 μg of brain homogenate was labeled for 1 h at RT with TAMRA-FP (1 μM) in a total volume of 25 μl. The reaction was stopped by adding 25 μl of 2 × SDS-loading buffer. The proteins were separated in SDS-electrophoresis gel (10%) together with molecular weight standards and TAMRA-FP-bound serine hydrolases were visualized by fluorescent scanning (λ_{ex} 552 nm; λ_{em} 575 nm) (Fujifilm FLA-3000 laser fluorescence scanner Fujifilm, Tokyo, Japan). The intensity of bands was quantified using ImageJ, freely available image analysis software (http://rsbweb.nih.gow/ij/).

2-AG-hydrolase activity assay

Total and MAGL-independent 2-AG-hydrolase activities of brain homogenates were determined by monitoring glycerol liberation from 2-AG hydrolysis by a fluorometric 96-well plate format assay, essentially as previously described (Navia-Paldanius et al., 2012; Aaltonen

et al., 2013). Briefly, for MAGL-independent and total activities, 1 µl of 10 µM JJKK-048 or DMSO, respectively, were preincubated with 99 µl of homogenates (1 µg/well) for 30 min at RT. Following this, 100 µl of assay mix containing the substrate 2-AG (50 µM final concentration) was added. The enzymatic glycerol production was coupled via a three-step enzymatic cascade to hydrogen peroxide (H_2O_2)-dependent generation of resorufin whose fluorescence (λ_{ex} 530; λ_{em} 590 nm) was kinetically monitored using a fluorescence plate reader (Tecan Infinite M200, Tecan Group Ltd., Männedorf, Switzerland).

Liquid chromatography-tandem mass spectrometry (LC-MS/MS)

Frozen brains were homogenized with Qiagen TissueLyser II (3 min with frequency 30 1/s) to obtain fine tissue powder. Approximately 10 mg of frozen tissue powder was weighted into microcentrifuge tubes. Extraction of the analytes from the sample matrix as well as the LC-MS/MS instrumentation and methods used in the endocannabinoid analysis have been previously described (Lehtonen et al., 2011; Aaltonen et al., 2014). For pharmacokinetic analysis a piece of frozen tissue was weighed and homogenized with water (1+3). An aliquot of 50 µL of the homogenate was taken and the proteins were precipitated with 150 µl of acetonitrile containing 0.1% formic acid (v/v) and the internal standard, diclofenac. The samples were vortexed and centrifuged at 4 °C, 14,000 × g for 10 min, after which the supernatant was taken for analysis. The JJKK-048 concentrations from tissue samples were analyzed with liquid chromatography-mass spectrometry. An Agilent 1200 Series Rapid Resolution LC System was used together with a Poroshell 120 EC-C-18 column (50 mm × 2.1 mm, 2.7 µm). A Rapid Resolution LC in-line filter (2 mm, max. 600 bar, 0.2 mm; Agilent Technologies) was used for protecting the analytical column from possible contaminants. The LC eluents were water (A) and acetonitrile (B), both containing 0.1% (v/v) formic acid. An

isocratic elution with 65 % B was applied for 4 minute with an eluent flow rate of 0.2 ml/min at column temperature 40°C and injection volume of 5 µl. The data were acquired with an Agilent 6410 Triple Quadrupole Mass Spectrometer equipped with an electrospray ionization source. The following mass spectrometry conditions were used: electrospray ionization, positive ion mode; drying gas (nitrogen) temperature, 300°C; drying gas flow rate, 10 l/min; nebulizer pressure, 40 psi; and capillary voltage, 4000 V. Analyte detection was performed using multiple reaction monitoring, the transitions being 435 → 366. The transition for the internal standard, diclofenac, was 296 → 250. Fragmentor voltage used for JJKK-048 was 60V and the collision energy was 5V. For diclofenac these parameters were 100V and 10V. The pressure of the collision cell nitrogen was adjusted to 2.9 10^{-5} Torr. The divert valve was programmed to allow eluent flow into the mass spectrometer from 0.5–4 minutes for each run. Agilent MassHunter Workstation Acquisition software (Data Acquisition for Triple Quadrupole Mass Spectometer, version B.03.01) was used for data acquisition, whereas Quantitative Analysis (B.04.00) software was used for the data processing and analysis. The lower limit of quantification for the brain and liver samples was 5 pmol/g and for plasma the lower limit of quantification was 1 nM. Linearity of the calibration curves were evaluated by a quadratic regression analysis. The method was also selective, accurate and precise over the calibration range. Within run accuracy and precision were calculated from the results of the quality control samples at the three concentrations. The accuracies and precisions for quality control concentrations of < 20 % were considered to be acceptable.

Behavioral experiments

Mice were evaluated in the tetrad test (locomotor activity, nociception in the writhing and tail immersion tests, catalepsy in the bar test, and hypothermia) for cannabimimetic effects.

Spontaneous locomotor activity was measured by means of a photocell apparatus (Multiserv, Poland). The number of photocell interruptions were recorded per each mouse for a total period of 10 min. Nociceptive reactions were studied in the acetic acid 'writhing' (Koster et al., 1959) and the tail immersion tests (Ben-Bassat et al., 1959). In the first test, the number of writhing episodes was measured for 10 min, starting 5 min after i.p. administration of acetic acid solution. In the second test, the animal's tail was placed in a water bath, heated to 52 °C and the latency of reflexive withdrawal was measured before injections of the drugs (baseline latency). Antinociceptive response was measured 30 min, 60 min, 90 min and 120 min after the JJKK-048 injection. The cut-off time was set to 20 s. Antinociceptive effects were expressed as the percent of maximum possible effect (%MPE), which was calculated according to the equation: $\%MPE = [(t_1 - t_0)/(20 - t_0)] \times 100\%$ (t_0 and t_1 are the pre-compound and post-compound latencies, respectively). Body temperature in normothermic mice was measured in animal's rectum with a thermistor thermometer. The mean value from the first two measurements (60 and 30 min before drug administration) was assumed as an initial temperature (ti). The final temperature (tf) was measured 120 min after JZL184 and 30 min after JJKK-048 administration or 30 min, 60 min and 120 min after the JJKK-048 injection. Body temperature changes (Δt) were calculated according to the formula: $\Delta t = tf - ti$. The catalepsy was measured using the bar test (120 min after JZL184 and 30 min after JJKK-048 administration): the front paws of each subject were placed on a cylindrical metal bar (0.75 cm diameter) that was elevated 4.5 cm above the table) and the time during which both forelimbs remained on the bar was recorded up to a maximum of 30 s. The test was repeated three times (inter-trial interval: 1 min). Animals were put back in their home cage after each measurement of catalepsy. Mice that remained motionless with their paws on the bar for 10 s (with the exception of respiratory movements) were scored as cataleptic (Little et al., 1988; Martin et al., 1991).

Data analysis

All the results are expressed either as mean + SEM, mean ± SEM or mean + SD, as indicated in the figures. In LC-MS/MS experiments and in quantification of the ABPP data, the statistical differences were determined using one-way ANOVA with Tukey's multiple comparison *post hoc* test. The results of behavioral experiments were calculated by two-way ANOVA (body temperature and tail immersion test) and one-way ANOVA (other tests) followed by Bonferroni's *post hoc* test. Specific paired comparison was performed with a Student's *t*-test when necessary. The comparisons of 2-AG hydrolase activities from brain samples were determined using unpaired *t*-test. In all experiments, $p<0.05$ was considered as statistically significant. All figures were prepared by using GraphPad Prism version 5.00 for Windows, GraphPad Software (San Diego, California, USA), www.graphpad.com.

Results

JJKK-048 potently inhibits MAGL and elevates brain 2-AG levels in mice

To test the *in vivo* effects of JJKK-048, male C57Bl/6J mice were treated with a dose range of 0.1-4 mg/kg (i.p.) of JJKK-048 or vehicle. After 30 min the mice were sacrificed, and their brains were removed for the analysis. Gel-based ABPP revealed a dose-dependent blockade of MAGL in brain (Figs. 1A and 1B). The dose as low as 0.5 mg/kg was found to produce partial (~45 %) blockade of MAGL, whereas with doses 1 and 2 mg/kg ~80 % and with 4 mg/kg ~90 % inhibition of MAGL was achieved (Figs. 1A and 1B). These findings demonstrate that JJKK-048 is an extremely potent MAGL inhibitor *in vivo*. In addition to MAGL-inhibition, the dose 0.5 mg/kg produced ~20 % blockade of ABHD6, whereas doses 1-2 mg/kg and 4 mg/kg produced ~60 % and ~85 % inhibition of ABHD6, respectively (Fig. 1A). Importantly, inhibition of FAAH or any additional serine hydrolases were not observed with any of the tested doses (Fig. 1A). We next measured the brain levels of 2-AG and AEA by LC-MS/MS. We found that JJKK-048 produced 9-fold elevations in brain 2-AG-levels with the dose 0.5 mg/kg and 19-fold elevations with doses 1 and 2 mg/kg when compared to control (Fig. 1C). 2-AG levels were increased up to 30-fold from the control with the dose 4 mg/kg. In contrast, brain AEA levels remained unaffected at all of the tested JJKK-048 doses (Fig. 1D). To further evaluate potent *in vivo* inhibition of MAGL demonstrated by ABPP (Figs. 1A and 1B), we quantified total and MAGL-independent 2-AG hydrolase activities of brain samples by a fluorescent glycerol assay. These results were in line with the ABPP observations as the MAGL-dependent 2-AG hydrolase activity was dose-dependently decreased when compared to vehicle (Fig. 1E,). With the doses 1-4 mg/kg of JJKK-048 the decrease was found statistically significant. On the other hand, *in vitro* incubation with JJKK-

048 (100 nM) significantly reduced activity with the vehicle and the JJKK-048 dose 0.1 mg/kg, indicating residual MAGL activity, whereas no significant reduction in MAGL-dependent 2-AG hydrolase activity was found with the doses from 0.5 to 4 mg/kg (Fig. 1E). These findings altogether confirm the dose-dependent inhibition of brain MAGL activity by JJKK-048 *in vivo*.

Next we assessed the duration of inhibition at various time points following a single dose of JJKK-048 (0.5 mg/kg, i.p.). In these conditions, competitive ABPP indicated a partial blockade (~45 %) of MAGL during the time period from 30 min to 2 hours after injection (Figs. 2A and 2B). Interestingly, MAGL activity returns close to the control level 4 hours after injection (Figs. 2A and 2B). Selectivity for MAGL over FAAH was maintained during the time course (Fig. 1A). Brain 2-AG levels were increased 2-fold from control already after 15 minutes and the highest brain 2-AG levels (9-fold increase from control) were observed 30 minutes after injection (Fig. 2C). The 2-AG levels were returned close to control levels 4 h after injection. AEA levels were unchanged throughout the studied time frame (Fig. 2D). In the glycerol assay, the 2-AG hydrolase activity was found significantly decreased during the time period from 1 to 2 hours after injection compared to vehicle (Fig. 2E, DMSO). *In vitro* incubation of samples with JJKK-048 (100 nM) further reduced the 2-AG hydrolase activity in vehicle and in time points 1 h and 4 h, indicating the presence of residual MAGL activity in these samples (Fig. 2E).

To evaluate the selectivity of JJKK-048 for MAGL in peripheral tissues, mice were treated with doses 0.5, 1 and 2 mg/kg of JJKK-048 or vehicle (i.p.), sacrificed 30 minutes after injection, and their tissues harvested. Competitive ABPP analysis was done using liver, spleen, heart and skeletal muscle samples. In these proteomes, a single (albeit weak) JJKK-

048-sensitive 33 kDa band was detected and identified as MAGL (Fig. 3). In brain, however, an additional 35 kDa form of MAGL was also observed corresponding to typical dual splice isoforms of MAGL (Figs. 1 and 2). In liver, JJKK-048 produced ~70 % MAGL inhibition with the dose 0.5 mg/kg with no detectable cross-reactivity with other serine hydrolases (Fig 3). With the doses 1 and 2 mg/kg, nearly complete (>90 %) inhibition of MAGL was evident, but with these doses, an off-target migrating ~ 70 kDa was detected (Fig. 3). In spleen, heart and skeletal muscle proteomes, ~30 % MAGL inhibition was achieved with the dose 0.5 mg/kg of JJKK-048 whereas doses 1 and 2 mg/kg resulted in >80 % MAGL inhibition (Fig. 3). Also in these proteomes, the doses 1 and 2 mg/kg inhibited a ~70 kDa enzyme (Fig. 3). Previously, JZL184 was demonstrated to have cross-reactivity with 50-65 kDa carboxylesterase (CES) enzymes in peripheral tissues (Long et al., 2009c; Chang et al., 2012). KML29 represented improved selectivity against CESs and only with high doses (20-40 mg/kg) blocked peripheral ~70 kDa enzyme, which was postulated to correspond to carboxylesterase 1 (ES1) (Chang et al, 2012). Due to structural similarities between KML29 and JJKK-048 it is likely, that ES1 is also the peripheral off-target of JJKK-048 in mice tissues in the present study.

Pharmacokinetic analysis of JJKK-048 in mice

After 0.5 mg/kg i.p. injection JJKK-048 was not detected from plasma or brain 15, 30, 60 or 120 min after the injection. Table 1 shows the JJKK-048 concentrations in plasma, brain and liver 30 min after the injection using 0.5 mg/kg, 1.0 mg/kg and 2.0 mg/kg doses.

JJKK-048 induces antinociception with minimal cannabimimetic side effects

It has been shown that direct CB_1 receptor agonists induce several behavioral effects in rodents, including thermal antinociception, hypomotility, hypothermia, and catalepsy. These typical cannabimimetic effects are often studied with a battery of tests referred to as the tetrad assay for cannabinoid activity (Little et al., 1988; Martin et al., 1991). Enhanced 2-AG signalling caused by MAGL inhibition has been found to elicit more modest effects in a tetrad assay than direct CB_1 agonism. For instance, MAGL inhibition by JZL184 elicited antinociception, hypomotility and hypothermia but not catalepsy (Long et al., 2009b). Since JJKK-048 was found to elevate brain 2-AG levels in our experiments, we were curious to learn if it is able to induce antinociception and other typical cannabimimetic behavioral effects. For comparison, we used JZL184 as a reference compound.

A significant reduction in motility of mice was observed 120 min after the administration of JZL184 (16 mg/kg, i.p.) and 30 min (but not 120 min) after the administration of JJKK-048 (0.5 mg/kg, i.p.) compared to the appropriate control group (Fig. 4A). A significant reduction in motility of mice was also observed after the injection of higher doses of JJKK-048 (1 and 2 mg/kg, i.p.) 30 min after the administration (Fig. 4B). Only the dose 2 mg/kg of JJKK-048 reduced motility 60 min and 120 min after the administration, when compared to the appropriate control group (Fig. 4B). The CB_1 receptor antagonist/inverse agonist rimonabant alone reduced motility of mice with doses 1 and 3 mg/kg when compared to the control group (Fig. 4C). Low dose of rimonabant (0.3 mg/kg) did not reduce motility on its own and this dose did not reverse action of JJKK-048 (1 mg/kg) when administered simultaneously. Surprisingly, co-administration of JJKK-048 (1 mg/kg) and rimonabant (1 mg/kg) induced an additive reduction in motility of mice versus the group injected with JJKK-048 alone (1 mg/kg) and versus the group with rimonabant alone (1 mg/kg) (Fig. 4C). The hypomotility

induced by 0.5 mg/kg of JJKK-048 (depicted in Fig. 4A) could not be repeated in the second experiment (Fig. 4C).

JJKK-048 (1 and 2 mg/kg) similarly to the reference compound, JZL184 (16 mg/kg, i.p.), significantly lowered body temperature of mice. Co-administration of ineffective dose of rimonabant (0.3 mg/kg) with JJKK-048 (1 mg/kg) could not reverse JJKK-048-induced decrease in body temperature (Fig. 5).

Next we tested analgesic effect of JZL184 and JJKK-048 with the acetic acid writhing test and with the tail immersion test. The writhing test is based on chemical stimulation by i.p. administration of agents that irritate serous membranes and provokes characteristic abdominal contractions. It is a model of visceral or peritoneal pain, although it does not preclude central mechanisms of antinociception (Koster et al., 1959; Le Bars et al., 2001). The tail-immersion test involves immersing the tail in water at a predetermined temperature provoking an abrupt movement of the tail; this is a spinal reflex and it does not affect visceral or musculoskeletal tissues (Le Bars et al., 2001). A significant reduction in the writhing episodes of mice was observed after the administration of JZL184 (16 mg/kg, i.p.) and JJKK-048 (0.5 and 1 mg/kg, i.p.) indicating analgesic effect of these compounds (Fig. 6A). JJKK-048 at higher dose (1 mg/kg) produced statistically significant action expressed as MPE compared to control group, indicating analgesic effect (Fig. 6D). What is more, this antinociceptive effect of JJKK-048 was comparable to the action of the reference cannabinoid agonist, WIN 55,212-2, in the tail immersion test (Fig. 6C). It should be noted that, administration of rimonabant (3 mg/kg) inhibited the effect of JJKK-048 indicating further that the observed analgesic effects in both tests are likely mediated by CB_1 receptors (Fig. 6B and 6C). The analgesic effect of JJKK-048 (1 mg/kg) in the tail immersion test lasted up to 120 min (Fig. 6C).

Finally, no cataleptic effects were observed after the injection of JZL184 (16 mg/kg i.p.) or JJKK-048 (0.5 mg/kg i.p.) when assessed with the bar test. According to the previous observations, half of the mice treated with a high dose of JZL184 (40 mg/kg) did exhibit hyperreflexia or “popcorning” behavior when presented with catalepsy bar apparatus (Long et al., 2009b) but these effects, however, were not observed with low inhibitor doses in our present study.

Discussion

During their existence, MAGL inhibitors have enabled functional investigation of 2-AG signaling pathways and revealed MAGL's role in physiological and pathophysiological processes. Sufficient potency and selectivity over other enzymes are required from an inhibitor intended to be used *in vivo*. Especially important is to achieve selectivity between MAGL and FAAH to avoid CB_1 agonist-like cataleptic behavior. Selective MAGL-inhibitors would provide means to treat conditions where increased 2-AG activity would be beneficial, including pain and neurodegenerative diseases.

JJKK-048 as a potent in vivo inhibitor of MAGL

Previously we described piperidine-based triazole urea JJKK-048 as being ultrapotent MAGL inhibitor with remarkable selectivity over other serine hydrolases and other endocannabinoid system targets (Aaltonen et al., 2013). We proposed that JJKK-048 inhibits MAGL in covalent manner by binding to the MAGL active site serine (S122), forming a carbamate adduct, and that the high potency of JJKK-048 is attributable to triazole leaving group (Aaltonen et al., 2013). In the present study we confirmed that JJKK-048 possesses remarkable potency also *in vivo*. Dose as low as 0.5 mg/kg partially inhibited MAGL in mice brain and also increased brain 2-AG levels 9-fold. With the dose 4 mg/kg, nearly complete MAGL inhibition was achieved. In comparison, JZL184 have been reported to inhibit 75% of mouse brain MAGL at the dose of 4 mg/kg whereas the dose 16 mg/kg resulted nearly complete inhibition of MAGL (Long et al., 2009b). With KML29, partial inhibition of MAGL was achieved with dose 5 mg/kg and maximal inhibition with 20 mg/kg (Chang et al., 2012). Thus JJKK-048 exhibits superior *in vivo* potency compared to JZL184 and KML29. In

contrast to JZL184 or KML29, that maintain their MAGL inhibition for several hours *in vivo* (Long et al., 2009b; Chang et al., 2012), duration of action of JJKK-048 was quite brief. In our previous *in vitro* study, JJKK-048 represented irreversible inhibition of MAGL up to 90 min (Aaltonen et al., 2013). The present *in vivo* findings, however, suggest a slowly reversible mechanism of action. The reversibility of JJKK-048 inhibition may be explained in part by the lack of steric hindrance of the carbamate adduct with the catalytic serine (Fig. 7). The slowly reversible mechanism of action has also been suggested for the related triazole-based MAGL inhibitor SAR629 (Bertrand et al., 2010). Reversible MAGL inhibition would be beneficial in drug development since side-effects related to irreversible inhibition could likely be avoided.

With high doses and when administered chronically, JZL184 has been displaying cross-reactivity with FAAH (Long et al., 2009b,c; Schlosburg et al., 2010) whereas KML29 maintained selectivity over FAAH (Chang et al., 2012). According to the present findings, JJKK-048 did not inhibit FAAH with any of the tested doses. This is consistent with the previous findings, where JJKK-048 showed >10 000-fold MAGL selectivity over FAAH (Aaltonen et al., 2013). Based on our previous observations, the bulky benzodioxolyl moieties, originally incorporated in the JZL184 chemical structure, are required for the high selectivity. Furthermore, the single bond linking the piperidine and benzodioxolyl moieties, present in chemical structure of JJKK-048, improves selectivity when compared to double bond. In the present study, the only off-target of JJKK-048 in the brain proteome was ABHD6. Also *in vitro*, ABHD6 was the closest off-target of both JJKK-048 (~630-fold hMAGL selectivity over hABHD6) (Aaltonen et al., 2013) and KML29 (>100-fold MAGL selectivity) (Chang et al., 2012). The active sites of MAGL and ABHD6 likely share common structural elements and previously we have been demonstrated that hMAGL and hABHD6

also share similar substrate preferences (Navia-Paldanius et al., 2012). With the dose 0.5 mg/kg, which produces partial blockade of MAGL, JJKK-048 proved to be relatively selective. It should be kept in mind that partial blockade of MAGL is more desirable for drugs since chronic pharmacological or genetic inactivation of MAGL results in 2-AG overflow and thereby, functional antagonism of the endocannabinoid system (Chanda et al., 2010; Schlosburg et al., 2010).

In liver, the low 0.5 mg/kg dose of JJKK-048 provided ~ 70 % inhibition of MAGL whereas in heart, spleen and skeletal muscle proteomes the dose 1 mg/kg was required for appreciable MAGL inhibition. Previously liver was found to be more sensitive to KML29 compared to brain and other organs (Pasquarelli et al., 2015). This phenomenon can likely be explained by high concentration of drug in liver after i.p. administration, as the drug is absorbed into the portal vein from the injection site. Our pharmacokinetic analysis for JJKK-048 was in accordance with this assumption. According to earlier findings for carbamate-based inhibitors (Ahn et al., 2007; Alexander and Cravatt, 2005; Zhang et al., 2007), JZL184 was found to inhibit 50-65 kDa CES enzymes in peripheral tissues (Long et al., 2009c). In our present study, JJKK-048 remained selectivity over majority of CESs in the studied proteomes. With the highest doses used, a ~70 kDa enzyme, which likely corresponds to ES1, was found to be the only peripheral off-target of JJKK-048.

Behavioral effects of JJKK-048 in mice

Classical tetrad test for cannabinoid activity includes determination of nociceptive behavior, locomotor activity, body temperature, and catalepsy (Little et al., 1988; Martin et al., 1991). Cannabinoid agonists induce all four tetrad effects i.e. analgesia, hypomotility, hypothermia

and catalepsy in rodents (Martin et al., 1991). In tetrad test, FAAH inhibitors generally induce analgesia but no cannabimimetic side effects (Kathuria et al., 2003; Long et al., 2009a) whereas dual inhibition of both MAGL and FAAH has been reported to induce all four tetrad effects (Long et al., 2009a). According to literature, MAGL-inhibitors represent somewhat varying effects in tetrad assay depending e.g. on the vehicle used (Long et al, 2009b,c; Ignatowska-Jankowska et al., 2014; Pasquarelli et al., 2015).

In this study, we tested the antinociceptive activity of the JJKK-048 by commonly used writhing test and the tail immersion test in mice (Le Bars et al., 2001). At the doses 0.5 and 1 mg/kg, JJKK-048 caused significant reduction in the writhing episodes of mice indicating antinociceptive effect. The antinociceptive effect of JJKK-048 in the writhing test was observed 30 min after administration, which was the time point when the peak 2-AG levels occurred. In the tail-immersion test, JJKK-048 showed antinociception only at 1 mg/kg dose, and it bore resemblance to the antinociception of WIN 55,212-2, the prototypic cannabinoid compound (Wiley et al., 2014). In both tests, pretreatment with rimonabant (3 mg/kg) blocked the antinociceptive action of JJKK-048, suggesting the involvement of CB_1 receptors. This is in accordance with the previous studies where CB_1 was found to mediate the antinociceptive effects of JZL184 in both warm water tail withdrawal and acetic acid stretching tests (Long et al., 2009b,c; Busquets-Garcia et al., 2011). Additionally, JJKK-048 substantially suppressed locomotor activity of mice at 1 and 2 mg/kg doses. In accordance with the literature (Long et al., 2009b; Compton et al., 1996), rimonabant alone reduced motility of mice at 1 and 3 mg/kg doses. Unexpectedly, co-administration of rimonabant (1 mg/kg) and JJKK-048 (1 mg/kg) reduced locomotion of mice in additive manner. Sigel et al. (2011) proved that an increase of 2-AG levels by JZL184 and simultaneous CB_1 receptor blockade by low concentrations of rimonabant resulted in hypomotility of wild type mice. These effects may

be caused by the direct molecular interaction between 2-AG and $GABA_A$ receptors. It has also been suggested that rimonabant can lead to a CB_1 receptor-mediated increase in GABA tone (Kim and Alger, 2010). JJKK-048 also reduced body temperature of mice and similarly to the effects observed in motility test, the effects were statistically significant for higher doses (1 and 2 mg/kg) and only in 30 min after injection. As reduction in locomotor activity and body temperature induced by JJKK-048 was not blocked by rimonabant, it may be that that these two effects of JJKK-048 are non-specific for CB1 receptors.

In accordance with previous findings with other MAGL inhibitors, JJKK-048 did not induce cataleptic effects. This was expected since previously catalepsy has only been observed following dual blockade of both FAAH and MAGL (Anderson et al., 2014). As both JJKK-048 and JZL184 exert effect through 2-AG, there seems to be discrepancy in the effects in mice. This is likely due to differences in the potency of the compounds and by the durance of the inhibitory effect, as JJKK-048 is reversible and JZL184 is an irreversible MAGL inhibitor.

Conclusions

Based on the present findings, JJKK-048 can be used to globally inactivate MAGL in both brain and peripheral tissues. JJKK-048 induced a massive increase in mouse brain 2-AG levels without affecting AEA levels. According to ABPP experiments, JJKK-048 remained selectivity over FAAH and the only off-target in brain was ABHD6. JJKK-048 appeared to be extremely potent MAGL inhibitor *in vivo*, exhibiting slowly reversible mechanism of action. Our results showed that JJKK-048 promoted significant analgesia in writhing test with the

low dose that did not cause cannabimimetic side effects. Higher dose of JJKK-048 induced analgesia both in writhing test and in tail immersion test, as well as hypomotility and hypothermia but not catalepsy. Based on these observations, JJKK-048 provides a potent pharmacological tool for the further functional characterization of MAGL.

Acknowledgments

We wish to thank Ms. Taija Hukkanen, Ms. Taina Vihavainen, Ms. Pirjo Hänninen, and Ms. Tiina Koivunen for excellent technical assistance. An essential support for behavioral study was provided by the Funds for the Statutory Activity of the Medical University of Lublin, Poland, what has been gratefully acknowledged.

Authorship contributions

Participated in research design: Aaltonen, Kedzierska, Orzelska-Górka, Lehtonen, Savinainen, Laitinen, Parkkari, and Gynther

Conducted experiments: Aaltonen, Kedzierska, Orzelska-Górka, Lehtonen, Navia-Paldanius, Jakupovic, and Gynther

Performed data analysis: Aaltonen, Kedzierska, Orzelska-Górka, Lehtonen, and Savinainen

Wrote or contributed to the writing of the manuscript: Aaltonen, Kedzierska, Orzelska-Górka, Savinainen, Nevalainen, Laitinen, Parkkari, and Gynther

References

Aaltonen N, Savinainen JR, Riera Ribas C, Rönkkö J, Kuusisto A, Korhonen J, Navia-Paldanius D, Häyrinen J, Takabe P, Käsnänen H, Pantsar T, Laitinen T, Lehtonen M, Pasonen-Seppänen S, Poso A, Nevalainen T, and Laitinen JT (2013) Piperazine and piperidine triazole ureas as ultrapotent and highly selective inhibitors of monoacylglycerol lipase. *Chem Biol* **20**: 379-390.

Aaltonen N, Riera Ribas C, Lehtonen M, Savinainen JR, and Laitinen JT (2014) Brain regional cannabinoid CB_1 receptor signalling and alternative enzymatic pathways for 2-arachidonoylglycerol generation in brain sections of diacylglycerol lipase deficient mice. *Eur J Pharm Sci* **51**: 87-95.

Ahn K, Johnson DS, Fitzgerald LR, Liimatta M, Arendse A, Stevenson T, Lund ET, Nugent RA, Nomanbhoy TK, Alexander JP, and Cravatt BF (2007) Novel mechanistic class of fatty acid amide hydrolase inhibitors with remarkable selectivity. *Biochemistry* **46**: 13019-13030.

Alexander JP and Cravatt BF (2005) Mechanism of carbamate inactivation of FAAH: implications for the design of covalent inhibitors and in vivo functional probes for enzymes. *Chem Biol* **12**: 1179-1187.

Anderson WB, Gould MJ, Torres RD, Mitchell VA, and Vaughan CW (2014) Actions of the dual FAAH/MAGL inhibitor JZL195 in a murine inflammatory pain model. *Neuropharmacology* **81**: 224-230.

Bar-On P, Millard CB, Harel M, Dvir H, Enz A, Sussman JL, and Silman I (2002) Kinetic and structural studies on the interaction of cholinesterases with the anti-Alzheimer drug rivastigmine. *Biochemistry* **41**: 3555-3564.

Ben-Bassat J, Peretz E, and Sulman FG (1959) Analgesimetry and ranking of analgesic drugs by the receptacle method. *Arch Int Pharmacodyn Ther* **122**: 434-447.

Berghuis P, Rajnicek AM, Morozov YM, Ross RA, Mulder J, Urbán GM, Monory K, Marsicano G, Matteoli M, Canty A, Irving AJ, Katona I, Yanagawa Y, Rakic P, Lutz B, Mackie K, and Harkany T (2007) Hardwiring the brain: endocannabinoids shape neuronal connectivity. *Science* **316**: 1212-1216.

Bertrand T, Augé F, Houtmann J, Rak A, Vallée F, Mikol V, Berne PF, Michot N, Cheuret D, Hoornaert C, and Mathieu M (2010) Structural basis for human monoglyceride lipase inhibition. *J Mol Biol* **396**: 663-673.

Bisogno T, Berrendero F, Ambrosino G, Cebeira M, Ramos JA, Fernandez-Ruiz JJ, and Di Marzo V (1999) Brain regional distribution of endocannabinoids: implications for their biosynthesis and biological function. *Biochem Biophys Res Commun* **256**: 377-380.

Blankman JL, Simon GM, and Cravatt BF (2007) A comprehensive profile of brain enzymes that hydrolyze the endocannabinoid 2-arachidonoylglycerol. *Chem Biol* **14**: 1347-1356.

Burston JJ, Sim-Selley LJ, Harloe JP, Mahadevan A, Razdan RK, Selley DE, and Wiley JL (2008) N-arachidonyl maleimide potentiates the pharmacological and biochemical effects of the endocannabinoid 2-arachidonylglycerol through inhibition of monoacylglycerol lipase. *J Pharmacol Exp Ther* **327**: 546-553.

Busquets-Garcia A, Puighermanal E, Pastor A, de la Torre R, Maldonado R, and Ozaita A (2011) Differential role of anandamide and 2-arachidonoylglycerol in memory and anxiety-like responses. *Biol Psychiatry* **70**: 479-486.

Chang JW, Niphakis MJ, Lum KM, Cognetta AB 3rd, Wang C, Matthews ML, Niessen S, Buczynski MW, Parsons LH, and Cravatt BF (2012) Highly selective inhibitors of monoacylglycerol lipase bearing a reactive group that is bioisosteric with endocannabinoid substrates. *Chem Biol* **19**: 579-588.

Chanda PK, Gao Y, Mark L, Btesh J, Strassle BW, Lu P, Piesla MJ, Zhang, MY, Bingham B, Uveges A, Kowal D, Garbe D, Kouranova EV, Ring RH, Bates B, Pangalos M, Kennedy JD, Whiteside GT, and Samad TA (2010) Monoacylglycerol lipase activity is a critical modulator of the tone and integrity of the endocannabinoid system. *Mol Pharmacol* **78**: 996-1003.

Chen R, Zhang J, Wu Y, Wang D, Feng G, Tang YP, Teng Z, and Chen C (2012) Monoacylglycerol lipase is a therapeutic target for Alzheimer's disease. *Cell Rep* **2**: 1329-1339.

Compton DR, Aceto MD, Lowe J, and Martin BR (1996) In vivo characterization of a specific cannabinoid receptor antagonist (SR141716A): inhibition of delta 9-tetrahydrocannabinol-induced responses and apparent agonist activity. *J Pharmacol Exp Ther* **277**: 586-594.

Deutsch DG and Chin SA (1993) Enzymatic synthesis and degradation of anandamide, a cannabinoid receptor agonist. *Biochem Pharmacol* **46**: 791-796.

Devane WA, Hanus L, Breuer A, Pertwee RG, Stevenson LA, Griffin G, Gibson D, Mandelbaum A, Etinger A, and Mechoulam R (1992) Isolation and structure of a brain constituent that binds to the cannabinoid receptor. *Science* **258**: 1946-1949.

Di Marzo V and Petrosino S (2007) Endocannabinoids and the regulation of their levels in health and disease. *Curr Opin Lipidol* **18**: 129-140.

Dinh TP, Carpenter D, Leslie FM, Freund TF, Katona I, Sensi SL, Kathuria S, and Piomelli D (2002) Brain monoglyceride lipase participating in endocannabinoid inactivation. *Proc Natl Acad Sci USA* **99**: 10819-10824.

Dinh TP, Kathuria S, and Piomelli D (2004) RNA interference suggests a primary role for monoacylglycerol lipase in the degradation of the endocannabinoid 2-arachidonoylglycerol. *Mol Pharmacol* **66**: 1260-1264.

Hashimotodani Y, Ohno-Shosaku T, and Kano M (2007) Endocannabinoids and synaptic function in the CNS. *Neuroscientist* **13**: 127-137.

Hohmann AG, Suplita RL, Bolton NM, Neely MH, Fegley D, Mangieri R, Krey JF, Walker JM, Holmes PV, Crystal JD, Duranti A, Tontini A, Mor M, Tarzia G, and Piomelli D (2005) An endocannabinoid mechanism for stress-induced analgesia. *Nature* **435**: 1108-1112.

Ignatowska-Jankowska BM, Ghosh S, Crowe MS, Kinsey SG, Niphakis MJ, Abdullah RA, Tao Q, O' Neal ST, Walentiny DM, Wiley JL, Cravatt BF, and Lichtman AH (2014) In vivo characterization of the highly selective monoacylglycerol lipase inhibitor KML29: antinociceptive activity without cannabimimetic side effects. *Br J Pharmacol* **171**: 1392-1407.

Karlsson M, Contreras JA, Hellman U, Tornqvist H, and Holm C (1997) cDNA cloning, tissue distribution, and identification of the catalytic triad of monoglyceride lipase. Evolutionary relationship to esterases, lysophospholipases, and haloperoxidases. *J Biol Chem* **272**: 27218-27223.

Kathuria S, Gaetani S, Fegley D, Valiño F, Duranti A, Tontini A, Mor M, Tarzia G, La Rana G, Calignano A, Giustino A, Tattoli M, Palmery M, Cuomo V, and Piomelli D (2003) Modulation of anxiety through blockade of anandamide hydrolysis. *Nat Med* **9**: 76-81.

Kim J and Alger BE (2010). Reduction in endocannabinoid tone is a homeostatic mechanism for specific inhibitory synapses. *Nat Neurosci* **13**: 592–600.

Koster R, Anderson M, and de Beer EJ (1959) Acetic acid for analgesic screening. *Fed Proc* **18**: 412-416.

Le Bars D, Gozariu M, and Cadden SW (2001) Animal models of nociception. *Pharmacol Rev* **53**: 597-652.

Lehtonen M, Storvik M, Malinen H, Hyytiä P, Lakso M, Auriola S, Wong G, and Callaway JC (2011) Determination of endocannabinoids in nematodes and human brain tissue by liquid chromatography electrospray ionization tandem mass spectrometry. *J Chromatogr B* **879**: 677–694.

Little PJ, Compton DR, Johnson MR, Melvin LS, and Martin BR (1988) Pharmacology and stereoselectivity of structurally novel cannabinoids in mice. *J Pharmacol Exp Ther* **247**: 1046-1051.

Long JZ, Nomura DK, Vann RE, Walentiny DM, Booker L, Jin X, Burston JJ, Sim-Selley LJ, Lichtman AH, Wiley JL, and Cravatt BF (2009a) Dual blockade of FAAH and MAGL identifies behavioral processes regulated by endocannabinoid crosstalk in vivo. *Proc Natl Acad Sci USA* **106**: 20270-20275.

Long JZ, Li W, Booker L, Burston JJ, Kinsey SG, Schlosburg JE, Pavón FJ, Serrano AM, Selley DE, Parsons LH, Lichtman AH, and Cravatt BF (2009b) Selective blockade of 2-arachidonoylglycerol hydrolysis produces cannabinoid behavioral effects. *Nat Chem Biol* **5**: 37-44.

Long JZ, Nomura DK, and Cravatt BF (2009c) Characterization of monoacylglycerol lipase inhibition reveals differences in central and peripheral endocannabinoid metabolism. *Chem Biol* **16**: 744-753.

Martin BR, Compton DR, Thomas BF, Prescott WR, Little PJ, Razdan RK, Johnson MR, Melvin LS, Mechoulam R, and Ward SJ (1991) Behavioral, biochemical, and molecular modeling evaluations of cannabinoid analogs. *Pharmacol Biochem Behav* **40**: 471-478.

Mechoulam R, Ben-Shabat S, Hanus L, Ligumsky M, Kaminski NE, Schatz AR, Gopher A, Almog S, Martin BR, Compton DR, Pertwee RG, Griffin G, Bayewitch M, Barg J, and Vogel Z (1995) Identification of an endogenous 2-monoglyceride, present in canine gut, that binds to cannabinoid receptors. *Biochem Pharmacol* **50**: 83-90.

Navia-Paldanius D, Savinainen JR, and Laitinen JT (2012). Biochemical and pharmacological characterization of human α/β-hydrolase domain containing 6 (ABHD6) and 12 (ABHD12). *J Lipid Res* **53**: 2413-2424.

Nomura DK, Morrison BE, Blankman JL, Long JZ, Kinsey SG, Marcondes MC, Ward AM, Hahn YK, Lichtman AH, Conti B, and Cravatt BF (2011) Endocannabinoid hydrolysis generates brain prostaglandins that promote neuroinflammation. *Science* **334**: 809-813.

Pacher P, Bátkai S, and Kunos G (2006) The endocannabinoid system as an emerging target of pharmacotherapy. *Pharmacol Rev* **58**: 389-462.

Pacher P and Kunos G (2013) Modulating the endocannabinoid system in human health and disease: successes and failures. *FEBS J* **280**: 1918-1943.

Pasquarelli N, Porazik C, Hanselmann J, Weydt P, Ferger B, and Witting A (2015) Comparative biochemical characterization of the monoacylglycerol lipase inhibitor KML29 in brain, spinal cord, liver, spleen, fat and muscle tissue. *Neuropharmacology* **91**: 148-156.

Piro JR, Benjamin DI, Duerr JM, Pi Y, Gonzales C, Wood KM, Schwartz JW, Nomura DK, and Samad TA (2012) A dysregulated endocannabinoid-eicosanoid network supports pathogenesis in a mouse model of Alzheimer's disease. *Cell Rep* **1**: 617-623.

Saario SM, Savinainen JR, Laitinen JT, Järvinen T, and Niemi R (2004) Monoglyceride lipase-like enzymatic activity is responsible for hydrolysis of 2-arachidonoylglycerol in rat cerebellar membranes. *Biochem Pharmacol* **67**: 1381–1387.

Saario SM, Salo OM, Nevalainen T, Poso A, Laitinen JT, Järvinen T, and Niemi R (2005) Characterization of the sulfhydryl-sensitive site in the enzyme responsible for hydrolysis of 2-arachidonoyl-glycerol in rat cerebellar membranes. *Chem Biol* **12**: 649-656.

Savinainen JR, Saario SM, and Laitinen JT (2012) The serine hydrolases MAGL, ABHD6 and ABHD12 as guardians of 2-arachidonoylglycerol signalling through cannabinoid receptors. *Acta Physiol* **204**: 267–276.

Schlosburg JE, Blankman JL, Long JZ, Nomura DK, Pan B, Kinsey SG, Nguyen PT, Ramesh D, Booker L, Burston JJ, Thomas EA, Selley DE, Sim-Selley LJ, Liu QS, Lichtman AH, and Cravatt BF (2010) Chronic monoacylglycerol lipase blockade causes functional antagonism of the endocannabinoid system. *Nat Neurosci* **13**: 1113-1119.

Sigel E, Baur R, Rácz I, Marazzi J, Smart TG, Zimmer A, and Gertsch J (2011) The major central endocannabinoid directly acts at GABAA receptors. *Proc Natl Acad Sci USA* **108**: 18150-18155.

Sugiura T, Kondo S, Sukagawa A, Nakane S, Shinoda A, Itoh K, Yamashita A, and Waku K (1995) 2-Arachidonoylglycerol: a possible endogenous cannabinoid receptor ligand in brain. *Biochem Biophys Res Commun* **215**: 89-97.

Sugiura T (2009) Physiological roles of 2-arachidonoylglycerol, an endogenous cannabinoid receptor ligand. *Biofactors* **35**: 88-97.

Wiley JL, Marisch JA, Huffman JW (2014) Moving around the molecule: Relationship between chemical structure and in vivo activity of synthetic cannabinoids. *Life Sciences* **27**:55-63.

Zhang D, Saraf A, Kolasa T, Bhatia P, Zheng GZ, Patel M, Lannoye GS, Richardson P, Stewart A, Rogers JC, Brioni JD, and Surowy CS (2007) Fatty acid amide hydrolase inhibitors display broad selectivity and inhibit multiple carboxylesterases as off-targets. *Neuropharmacology* **52**: 1095-1105.

Footnotes

This work was supported by Academy of Finland [Grants 139140, 139620, 278212]; Finnish Cultural Foundation; and Funds for Statutory Activity of Medical University of Lublin, Lublin, Poland [DS 21/2014].

Figure legends

Figure 1

Dose-dependent JJKK-048 activity in mouse brain. (A-B) ABPP of serine hydrolases in mouse brain homogenate proteome using the TAMRA-FP probe. Mice were treated with JJKK-048 at the indicated dose range (0.1-4 mg/kg, i.p.) and sacrificed 30 min after injection. Molecular weight markers are indicated at left. (B) Quantitative data (mean + SEM) on the effect of JJKK-048 on probe labelling of the MAGL doublet. Data are derived from three separate ABPP experiments, ***$p<0.001$. (C-D) Brain levels of 2-AG and AEA across the indicated dose range of JJKK-048 (0.1-4 mg/kg, i.p., 30 min). Brain tissue was homogenized and extracted with chloroform-methanol followed by analysis with LC-MS/MS. Data are presented as mean + SEM, n = 3-6 animals/group, ***$p<0.001$. (E) Glycerol assay reveals dose-dependent loss of MAGL activity in brain samples of mice treated with JJKK-048 (0.1-4 mg/kg, i.p.). Data are presented as mean + SEM, n = 3-4 animals/group. An asterisk denotes a significant MAGL-dependent *in vitro* inhibition by 100 nM JJKK-048, (** $p<0.005$). A hashtag (#) indicates a significant difference in activity (*in vitro* DMSO) compared to control treatment (vehicle), # $p<0.05$, ## $p<0.01$.

Figure 2

Time course analysis of MAGL inactivation by JJKK-048 in mouse brain. (A-B) ABPP of serine hydrolases in mouse brain homogenate proteome using the TAMRA-FP probe. Mice were treated with 0.5 mg/kg (i.p.) of JJKK-048 and sacrificed after the indicated time. Molecular weight markers are indicated at left. (B) Quantitative data (mean + SEM) on the effect of JJKK-048 on probe labelling of the MAGL doublet. Data are derived from three

separate ABPP experiments, * $p<0.05$, ** $p<0.01$. (C-D) Brain levels of 2-AG and AEA followed by treatment of 0.5 mg/kg (i.p.) of JJKK-048 for the indicated time period. Brain tissue was homogenized and extracted with chloroform-methanol followed by analysis with LC-MS/MS. Data are presented as mean + SEM, n = 4-6 animals/group, ***$p<0.001$. (E) MAGL-dependent brain 2-AG hydrolase activity from mice treated with JJKK-048 (0.5 mg/kg, i.p, 30 min - 4 h). Data are presented as mean + SD, n = 2 animals/group. An asterisk denotes a significant MAGL-dependent *in vitro* inhibition by 100 nM JJKK-048, (* $p<0.05$, ** $p<0.005$). A hashtag (#) indicates a significant difference in activity (*in vitro* DMSO) compared to control treatment (vehicle), # $p<0.05$.

Figure 3

ABPP of serine hydrolase activities in mouse liver, spleen, heart, and skeletal muscle proteomes using the TAMRA-FP probe. Mice were treated with the indicated dose range (0.5-2 mg/kg, i.p.) of JJKK-048 and sacrificed after 30 min. Molecular weight markers are indicated at left. The image is representative from two ABPP experiments with similar outcome.

Figure 4

Effects of JJKK-048 and JZL184 on locomotor activity in mice. (A) A significant reduction in motility of mice is observed after the administration of JZL184 (16 mg/kg, i.p.) and JJKK-048 (0.5 mg/kg, i.p.) compared to the appropriate control group. JJKK-048 reduces locomotion 30 min but not 120 min after administration. (B) Doses 1 and 2 mg/kg (i.p.) of JJKK-048 reduce motility of mice 30 min after the administration whereas only 2 mg/kg of JJKK-048 reduces

motility of mice 60 and 120 min after the administration compared to the appropriate control group. (C) JJKK-048 (1 and 2 mg/kg, i.p.) and Rimonabant (Rim) (1 and 3 mg/kg, i.p.) induce a significant reduction in motility of mice compared to the control group. Co-administration of JJKK-048 (1 mg/kg) and Rim (1 mg/kg) decreased motility of mice in additive manner versus the group injected with JJKK-048 (1 mg/kg) and versus the group with Rim (1 mg/kg). Rim was injected 40 min before the test. In the case of co-administration, JJKK-048 was injected 30 min before the observation. Locomotor activity was measured for a period of 10 min. Data are expressed as mean + SEM values. *, # $p<0.05$; **, ## $p<0.01$ and ***, ^^^ $p<0.001$ (Bonferroni's test). Control I = DMSO/HP-β-CD; Control II = 4:1 v/v PEG 300/ Tween 80.

Figure 5

Determination of body temperature of mice after i.p. administration of JKK-048 and JZL184. JZL184 (16 mg/kg) and JJKK-048 (1 and 2 mg/kg) significantly lower the body temperature of mice whereas JJKK-048 (0.5 mg/kg) has no effect. Rim at the ineffective dose of 0.3 mg/kg does not reverse JJKK-048-induced decrease in body temperature. Body temperature was measured 120 min after JZL-184 and 30 min after JJKK-048 administration. Data are expressed as mean ± SEM values. *$p<0.05$; ***$p<0.001$ (Bonferroni's test). Control I = DMSO/HP-β-CD; Control II = 4:1 v/v PEG 300/ Tween 80.

Figure 6

The effects of JJKK-048 and JZL184 on nociceptive reactions in the writhing test and in the tail immersion test in mice. (A) A significant reduction in the writhing episodes of mice is

observed after the administration of JZL184 (16 mg/kg, i.p.) and JJKK-048 (0.5 and 1 mg/kg, i.p.). Administration of rimonabant (Rim) (3 mg/kg, i.p.) inhibits antinociceptive effect of JJKK-048 in the writhing (B) and tail immersion (C) tests. For A and B, the number of writhing episodes was measured for 10 min, starting 5 min after i.p. administration of acid solution. JZL184 was injected 120 min, JJKK-048 30 min and acetic acid (0.6 % solution) 5 min before the test. Antinociceptive response was measured 120 min after JZL184 and 30 min after JJKK-048 administration. (C) JJKK-048 at the dose 1 mg/kg (i.p.) and WIN 55,212-2 show antinociceptive response in the tail immersion test 30 min, 60 min, 90 min and 120 min after the injection. %MPE - the percent of maximum possible effect. Data are expressed as mean + SEM or mean ± SEM values. *, #, ^ $p<0.05$ and **, ^^ $p<0.01$, ***, ^^^ $p<0.001$ (Bonferroni's test). Control I = DMSO/HP-β-CD; Control II = 4:1 v/v PEG 300/ Tween 80.

Figure 7

Hydrolysis of JKK-048 (**a**) and JZL184/KML29 (**b**) carbamate adduct. The carbamate adducts (**1a-b**) can be released through hydrolysis and the released carbamic acid (**2a-b**) is then assumed to spontaneously break down to the corresponding amine (**3**) and carbon dioxide. JJKK-048 differ from analogues JZL184 and KML29 only by the hydroxyl group which is present in JZL184 and KLM29 but absent from JJKK-048. The acidicity of leaving groups cannot explain the reversibility of JJKK-048 as the hydroxyl group has practically no effect on acidicity of the carbamic acids **2a** and **2b**. However, the slightly larger size of JZL184/KLM29 carbamate adduct **1b** may cause a steric hindrance, preventing the attack by water oxygen to the carbonyl carbon, making the JJKK-048 carbamate adduct **1a** slightly more susceptible for hydrolysis when compared to JZL184/KLM29.

Tables

Table 1. JJKK-048 concentration in plasma, brain and liver 30 min after i.p. injection at 0.5 mg/kg, 1.0 mg/kg and 2.0 mg/kg doses.

	Plasma (μM)	Brain (nmol/g)	Liver (nmol/g)
0.5 mg/kg	[a]	[a]	0.047 ± 0.025
1.0 mg/kg	0.003 ± 0.00	0.017 ± 0.001	0.500 ± 0.088
2.0 mg/kg	0.175 ± 0.01	0.125 ± 0.174	0.666 ± 0.330

[a] concentrations below lower limit of detection

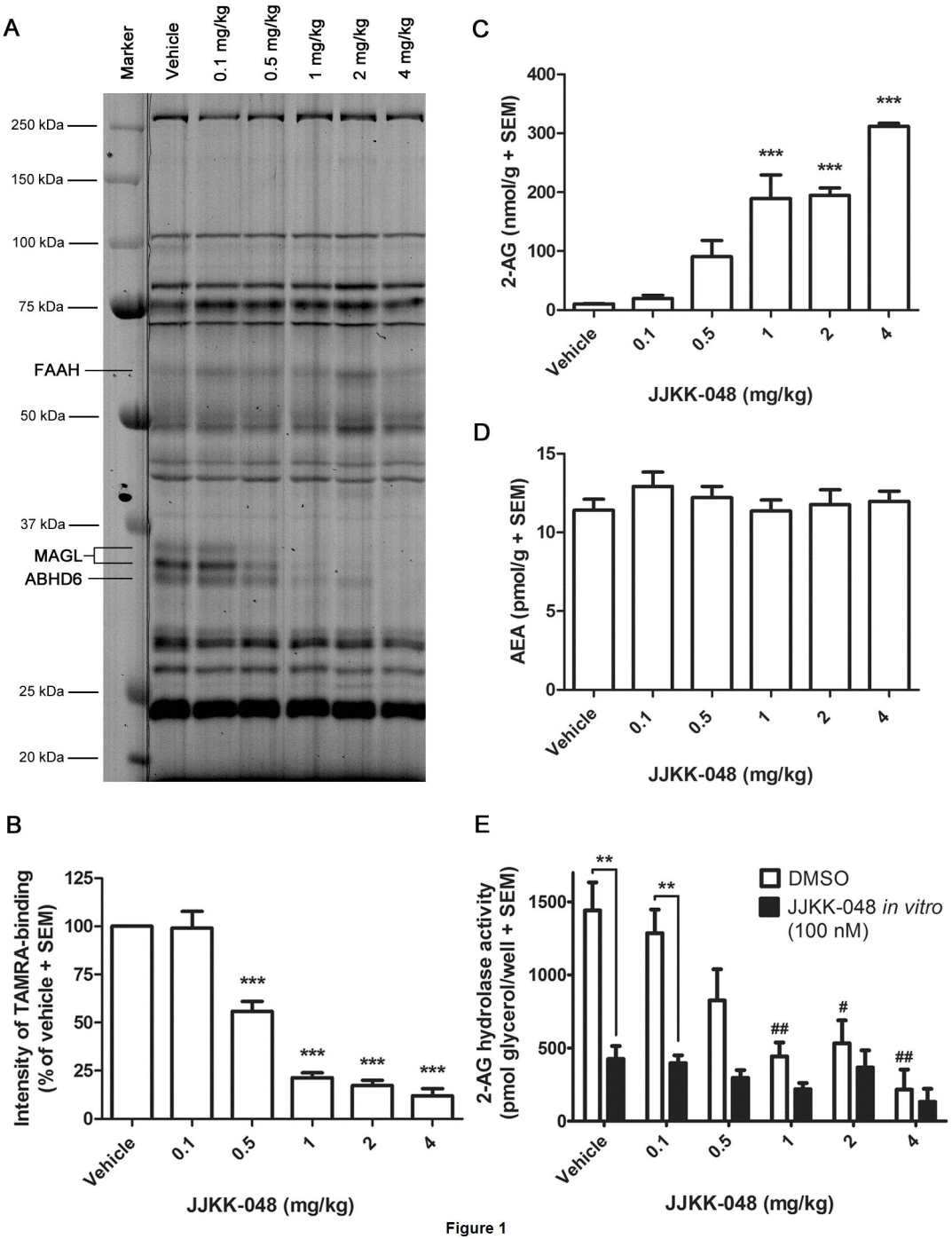
A
Marker
Vehicle
0.1 mg/kg
0.5 mg/kg
1 mg/kg
2 mg/kg
4 mg/kg
250 kDa
150 kDa
100 kDa
75 kDa
FAAH
50 kDa
37 kDa
MAGL
ABHD6
25 kDa
20 kDa
C
2-AG (nmol/g + SEM)
400
300
200
100
0
***
***
***
Vehicle
0.1
0.5
1
2
4
JJKK-048 (mg/kg)
D
AEA (pmol/g + SEM)
15
10
5
0
Vehicle
0.1
0.5
1
2
4
JJKK-048 (mg/kg)
B
Intensity of TAMRA-binding (% of vehicle + SEM)
125
100
75
50
25
0
***
***
***
Vehicle
0.1
0.5
1
2
4
JJKK-048 (mg/kg)
E
2-AG hydrolase activity (pmol glycerol/well + SEM)
1500
1000
500
0
**
**
##
#
##
DMSO
JJKK-048 in vitro (100 nM)
Vehicle
0.1
0.5
1
2
4
JJKK-048 (mg/kg)

Figure 1

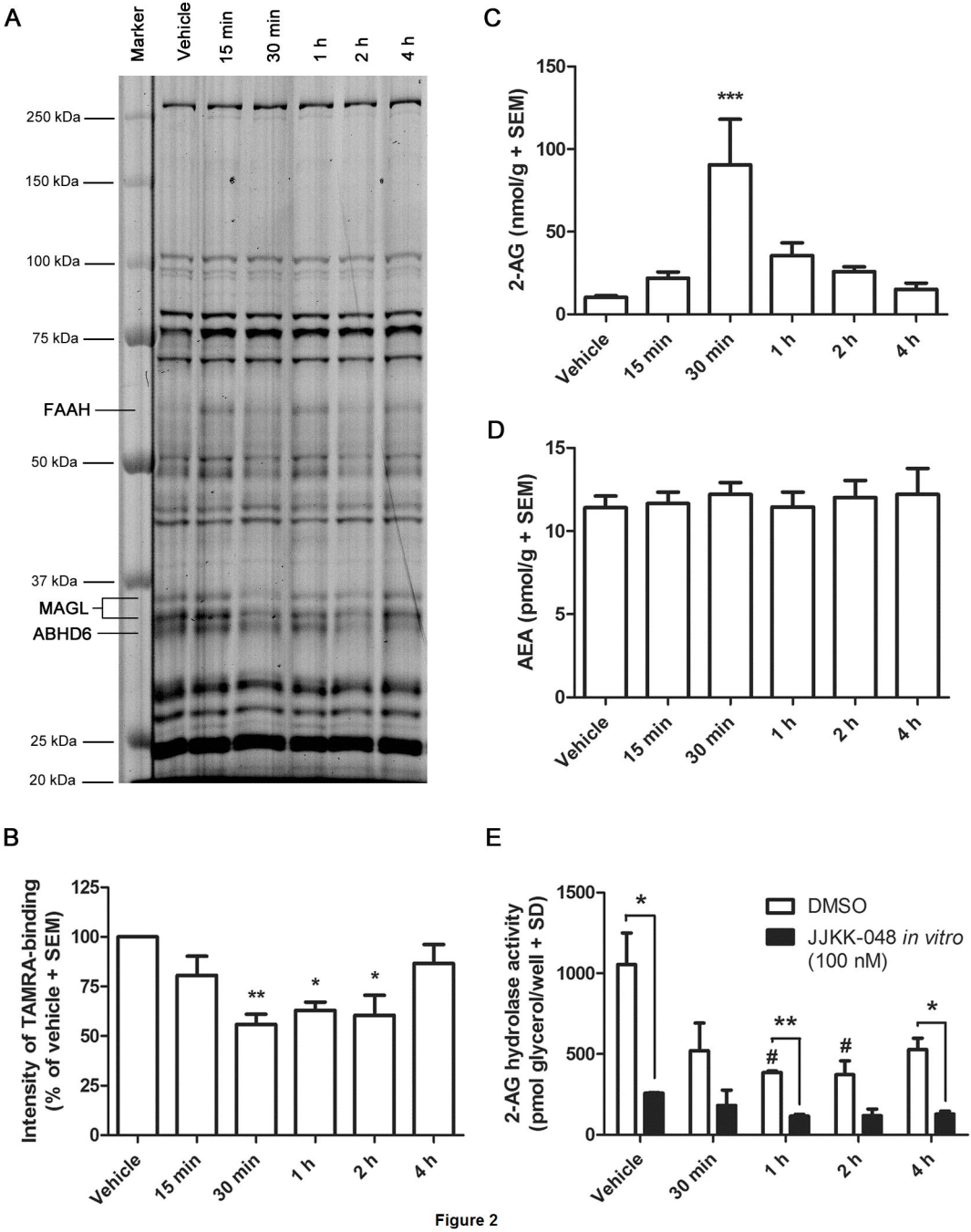
A
Marker
Vehicle
15 min
30 min
1 h
2 h
4 h
250 kDa
150 kDa
100 kDa
75 kDa
FAAH
50 kDa
37 kDa
MAGL
ABHD6
25 kDa
20 kDa
C
2-AG (nmol/g + SEM)
***
D
AEA (pmol/g + SEM)
B
Intensity of TAMRA-binding (% of vehicle + SEM)
E
2-AG hydrolase activity (pmol glycerol/well + SD)
DMSO
JJKK-048 in vitro (100 nM)

Figure 2

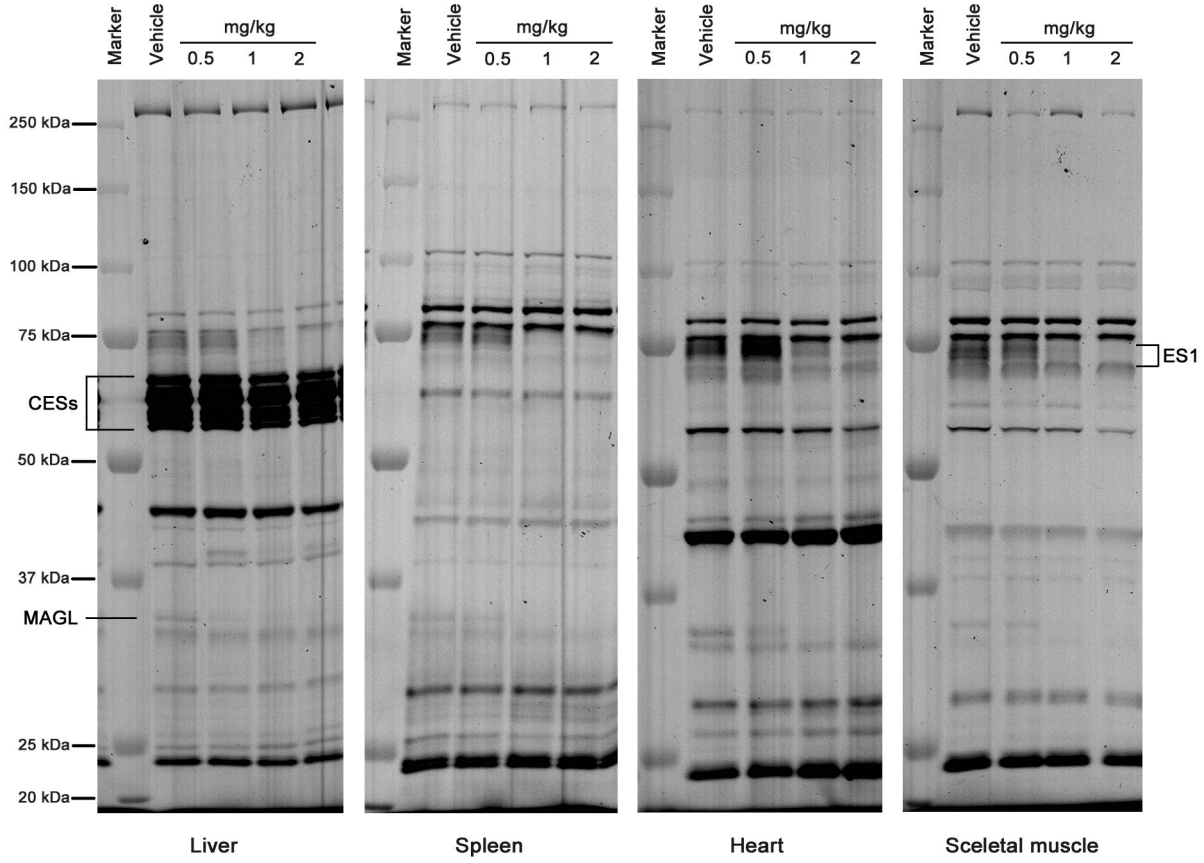
Marker
Vehicle
mg/kg
0.5
1
2
250 kDa
150 kDa
100 kDa
75 kDa
CESs
50 kDa
37 kDa
MAGL
25 kDa
20 kDa
ES1
Liver
Spleen
Heart
Sceletal muscle

Figure 3

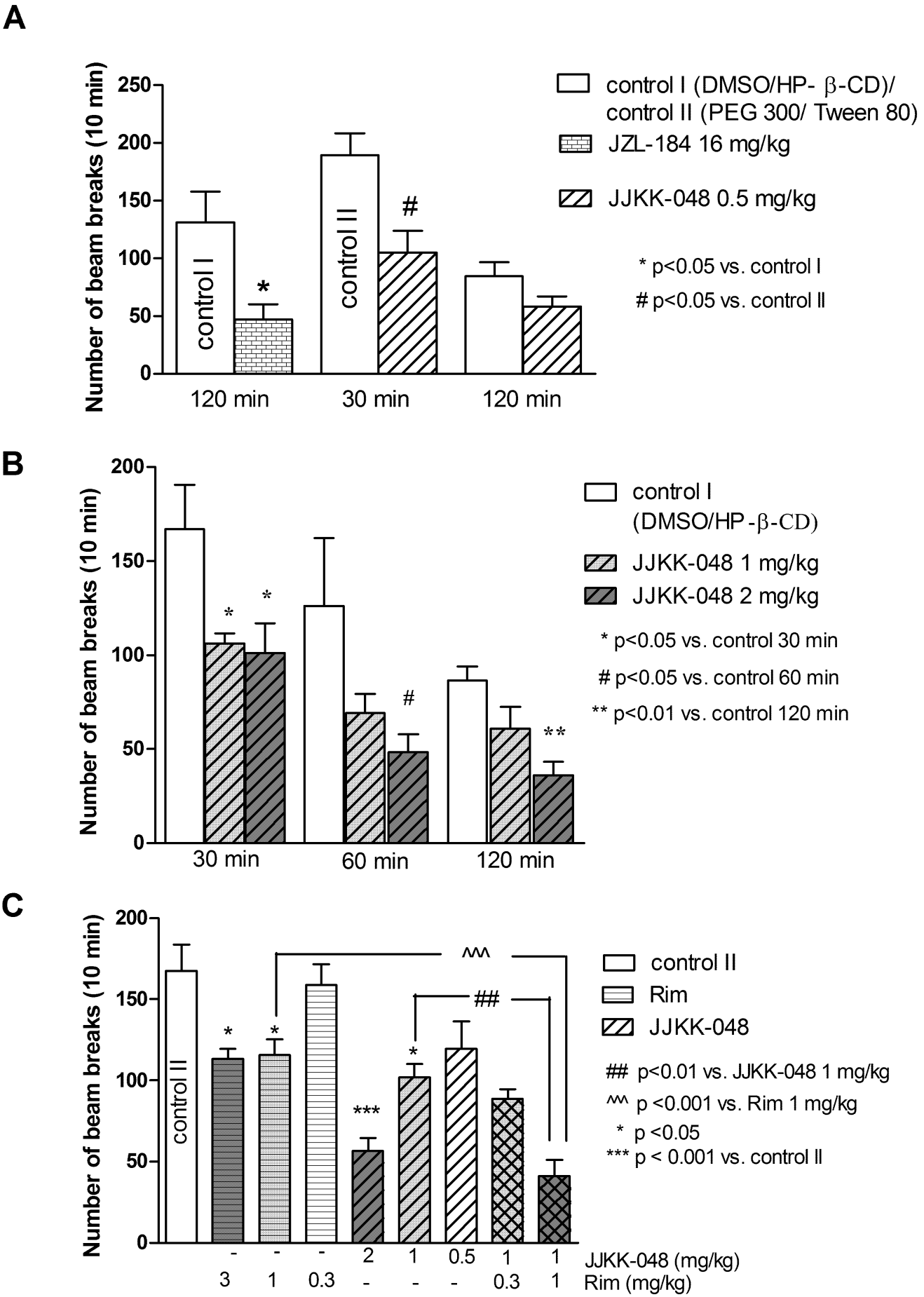
A
Number of beam breaks (10 min)
250
200
150
100
50
0
control I
control II
*
#
120 min
30 min
120 min
control I (DMSO/HP- β-CD)/
control II (PEG 300/ Tween 80)
JZL-184 16 mg/kg
JJKK-048 0.5 mg/kg
* p<0.05 vs. control I
# p<0.05 vs. control II
B
Number of beam breaks (10 min)
200
150
100
50
0
*
*
#
**
30 min
60 min
120 min
control I
(DMSO/HP-β-CD)
JJKK-048 1 mg/kg
JJKK-048 2 mg/kg
* p<0.05 vs. control 30 min
# p<0.05 vs. control 60 min
** p<0.01 vs. control 120 min
C
Number of beam breaks (10 min)
200
150
100
50
0
control II
*
*
***
*
^^
##
- - - 2 1 0.5 1 1
JJKK-048 (mg/kg)
3 1 0.3 - - - 0.3 1
Rim (mg/kg)
control II
Rim
JJKK-048
p<0.01 vs. JJKK-048 1 mg/kg
^^ p <0.001 vs. Rim 1 mg/kg
* p <0.05
*** p < 0.001 vs. control II

Figure 4.

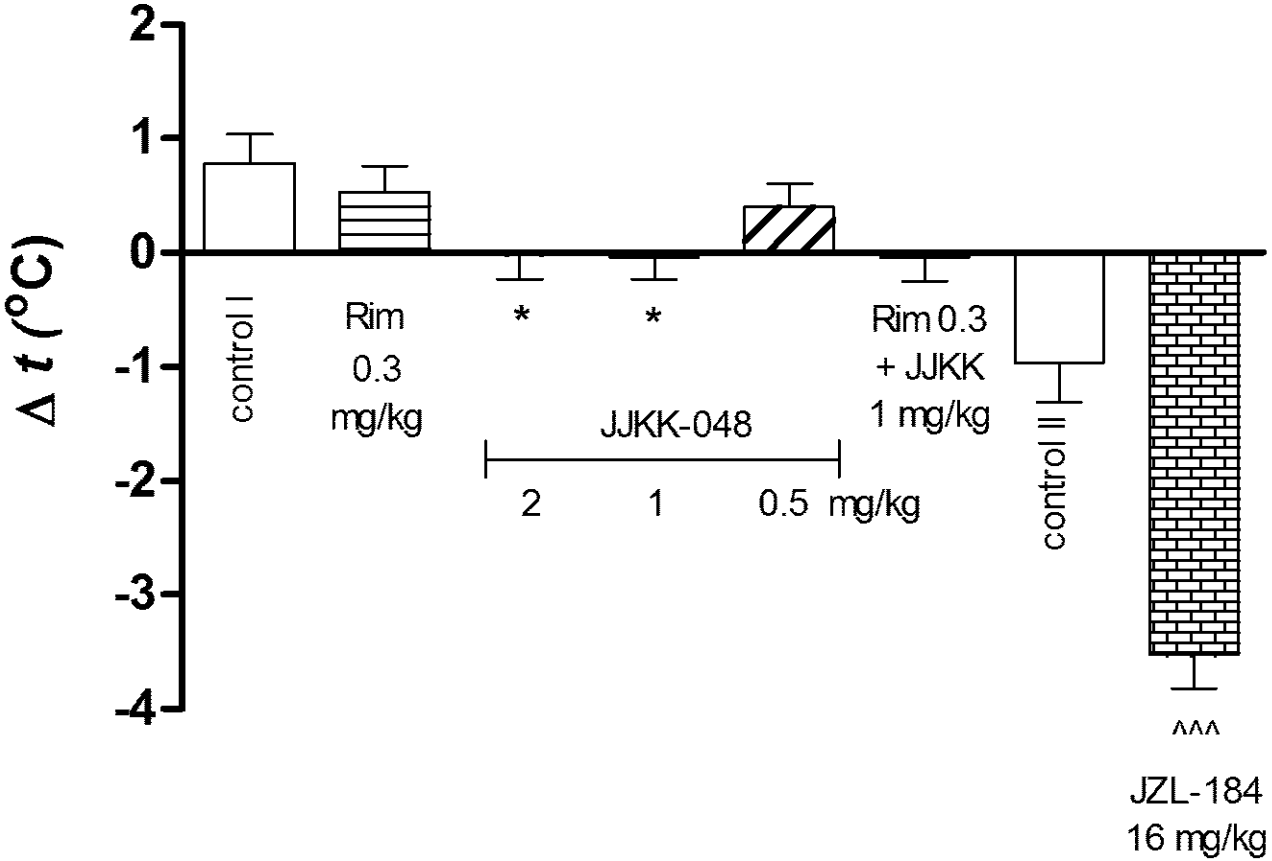

* - p<0.05;
vs. control I
(DMSO/HP-B-CD)

^^^ - p<0.001
vs. control II
(PEG300/Tween80)

Figure 5

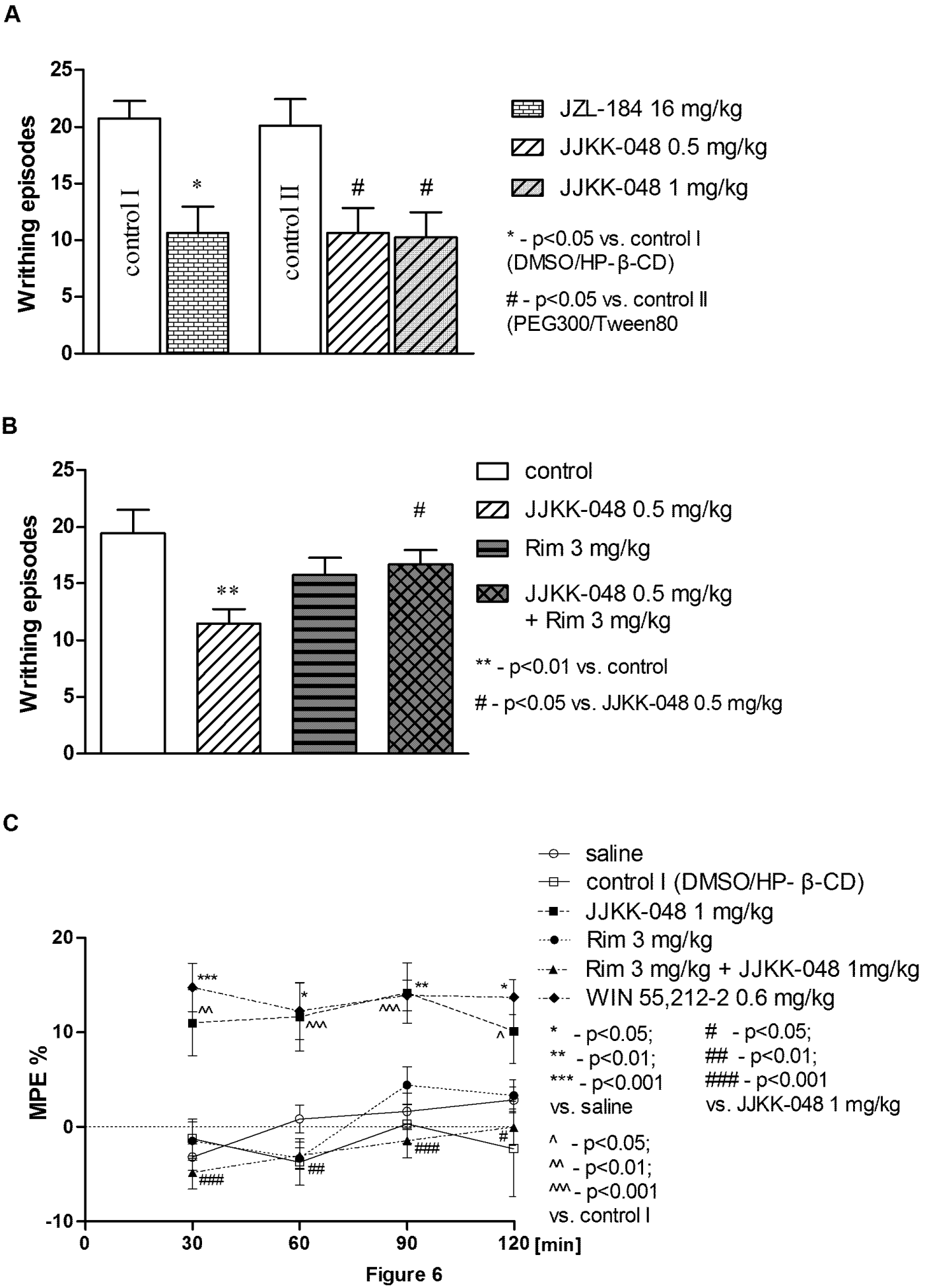
A
Writhing episodes
25
20
15
10
5
0
control I
control II
*
#
#
JZL-184 16 mg/kg
JJKK-048 0.5 mg/kg
JJKK-048 1 mg/kg
* - p<0.05 vs. control I
(DMSO/HP-β-CD)
- p<0.05 vs. control II
(PEG300/Tween80
B
Writhing episodes
25
20
15
10
5
0
**
#
control
JJKK-048 0.5 mg/kg
Rim 3 mg/kg
JJKK-048 0.5 mg/kg
+ Rim 3 mg/kg
** - p<0.01 vs. control
# - p<0.05 vs. JJKK-048 0.5 mg/kg
C
MPE %
20
10
0
-10
0
30
60
90
120
[min]
saline
control I (DMSO/HP- β-CD)
JJKK-048 1 mg/kg
Rim 3 mg/kg
Rim 3 mg/kg + JJKK-048 1mg/kg
WIN 55,212-2 0.6 mg/kg
* - p<0.05;
** - p<0.01;
*** - p<0.001
vs. saline
- p<0.05;
- p<0.01;
- p<0.001
vs. JJKK-048 1 mg/kg
^ - p<0.05;
^^ - p<0.01;
^^^ - p<0.001
vs. control I

Figure 6

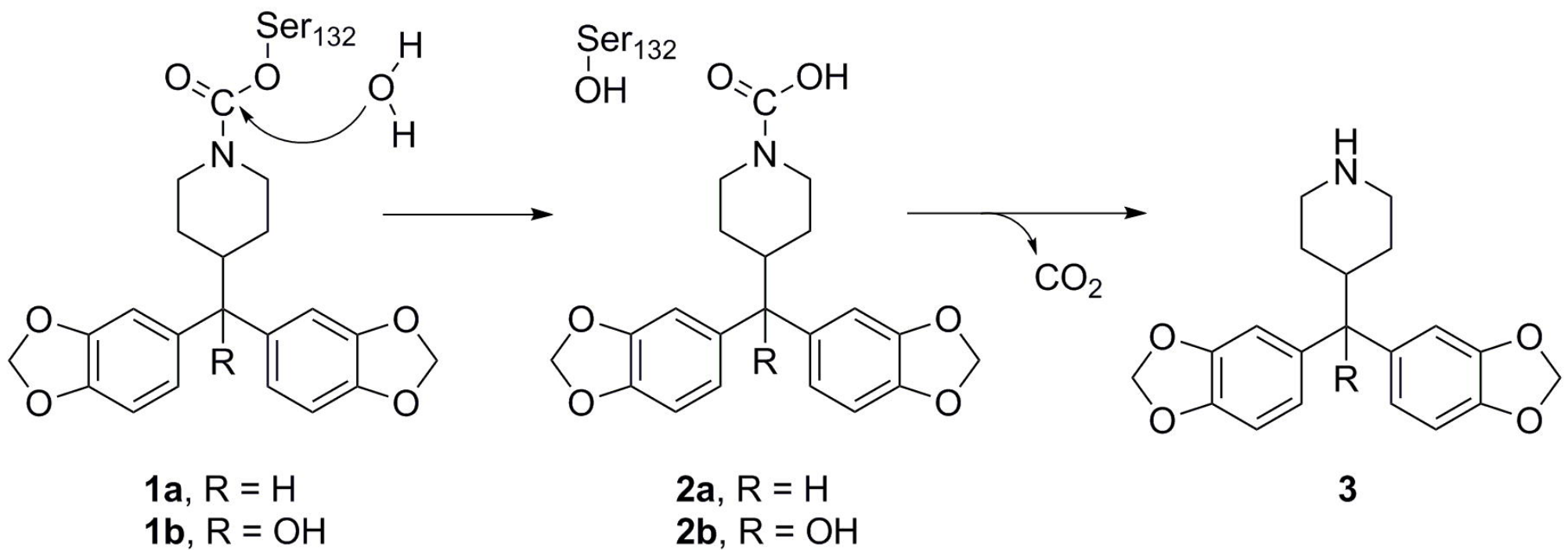

1a, R = H
1b, R = OH

2a, R = H
2b, R = OH

3

Figure 7